SAND2007-1188C

Microfluidics and Microacoustics for Miniature Flow Cytometry

Surendra K. Ravula*, Darren W. Branch*, Paul Clem*, Gregory Kaduchak**, Igal Brener*

Sandia National Labs, Albuquerque, NM, 87123, skravul@sandia.gov
Los Alamos National Labs, Los Alamos, NM 87545, kaduchak@lanl.gov

ABSTRACT

Flow cytometry is an indispensable tool in clinical diagnostics, for example in cancer, AIDS, infectious disease outbreaks, microbiology, and others. The cost and size of existing cytometers precludes their entry into field clinics, water monitoring, agriculture/veterinary diagnostics, and rapidly deployable biothreat detection. Much of the cost and footprint of conventional cytometers is dictated by the high speed achieved by cells or beads in a hydrodynamically focused stream. This constraint is removed by using ultrasonic focusing in a parallel microfluidic architecture. In this paper, we describe our progress towards a microfabricated flow cytometer that uses bulk and microfabricated planar piezoelectric transducers in glass microfluidic channels. In addition to experimental data, initial modeling data to predict the performance of our transducers are discussed.

Keywords: microfluidics, microacoustics, flow cytometry

1 INTRODUCTION

Over the last fifty years, commercial flow cytometers have become commonplace in clinical and laboratory settings for cellular analyses; however, these complex systems are bulky and expensive. Recently, flow cytometry systems based on microfluidics have brought hope for less expensive and portable alternatives to conventional systems [1-6]. These systems take advantage of the ability of microtechnology to pattern small features and integrate multiple sensing modalities (optical, electrical, mechanical) onto a single platform. In addition, microfluidics offers the ability to build complex interrogation channels that can focus cells into narrow single-file columns for downstream optical interrogation. However, underlying issues (e.g., cell clumping, adhesion to the channel) with appropriate routing of the particles to necessary points in an integrated system remain problematic. Here, we seek to address some of these issues by integrating acoustic standing waves into microfluidic channel systems to focus particles for optical detection.

2 METHODS

The integrated system starts with an alumina substrate on which platinum is deposited (thickness 2000 Å) for the ground electrode. On top of this electrode, PZT is aerosol deposited and heat treated (900ºC) to obtain a 75µm thick film. Finally, the top platinum electrode is patterned via DC sputtering (thickness=2000 Å) with a shadow mask to complete the circuit that actuates the PZT (see Figure 1a). Alternately, 1.5in. diameter circular PZT discs were sputtered with Cr/Au (200Å/2000Å) on both sides and lithographically patterned on the top side. In this approach, AZ 5740 photoresist was spin coated (Headway Research Inc., Garland, TX) at 5000rpm for 30s (~6µm thickness) and soft baked for 10min at 90°C. An optical aligner (Oriel Corporation, Stanford, CT) was used to expose the photoresist and was subsequently developed in Microposit 454 developer (Rohm and Haas, Philadelphia, PA). Finally, liftoff was used to remove the photoresist and pattern the top metal surface (see Figure 1b). A third technique used a bulk PZT (Sensor Technologies Limited, CA) glued to the underside of the microchannel structure (see Figure 1c).

For the patterned PZT structures, the transducer was poled at 300V DC to actuate in the thickness dimension. In each case, a glass microchannel (Micronit Microfluidics BV, Netherlands) is bonded to provide the conduit for microparticle flow and the area where an acoustic standing wave can be created (see Figures 2 and 3). Finally, the

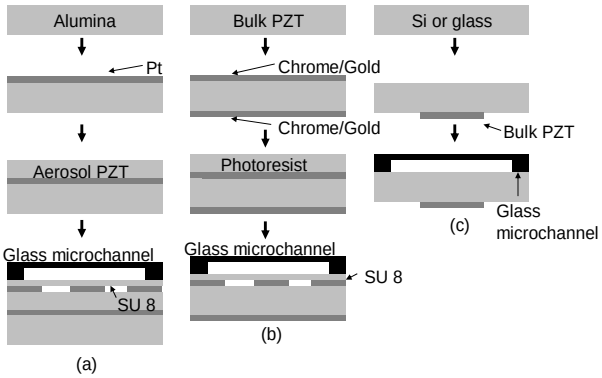

Figure 1. Fabrication schemes for the integrated flow cytometry system. (a) In the first scheme, platinum is deposited on an alumina substrate with a DC sputterer. Then an aerosol PZT is sprayed and heat treated on the substrate. Finally, a top electrode is patterned through a shadow mask using the sputterer. (b) In the second scheme, a 1.5in. PZT disc (500µm thick) is patterned with a top electrode metal layer using a liftoff procedure. (c) In the third scheme, a bulk PZT (pre-electroded) is glued to the underside of a Si substrate. In the first two cases, SU 8 2010 is spun on the top electrode and a glass microfluidic channel is pressure/heat bonded to the transducer. In the third case, a microfluidic channel is anodically bonded to the substrate.

system is fitted with tubing at the inlet and outlet to provide continuous delivery of 20µm diameter polystyrene beads (Sigma Aldrich, St. Louis, MO) via a syringe pump. When beads were tested in the system (for the case in Figure 1c), the PZT is driven at an amplitude of 10-20V_{p-p} and at 1MHz with an Agilent 33250A function generator connected to a power amplifier.

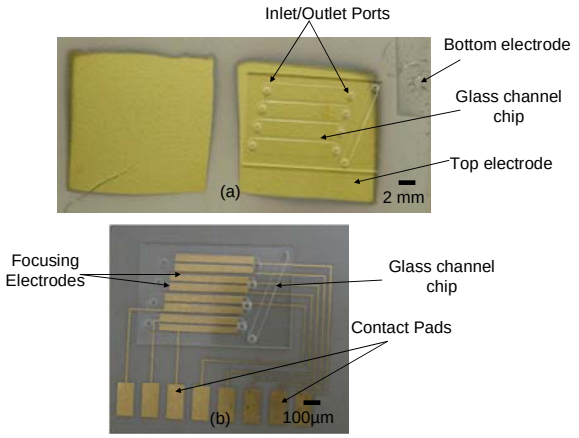

Figure 2. Fabricated patterned PZT approaches for integrated flow cytometry system. (a) The fabrication scheme in Figure 1a is used to pattern the top electrode on aerosol PZT. (b) The fabrication scheme used in Figure 1b is used to pattern the top electrode on bulk PZT. In both cases, a microchannel chip is bonded to the top using SU 8 photoresist.

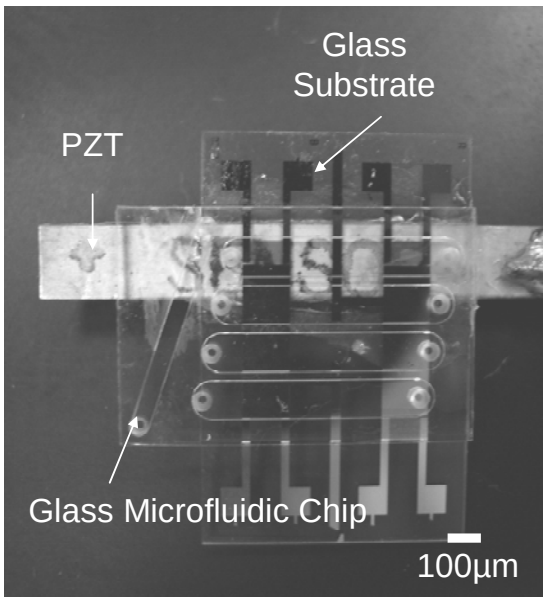

Figure 3. The fabrication scheme in Figure 1c is used to attach a bulk PZT (pre-electroded) to a glass substrate that is bonded to the microfluidic chip.

3 ACOUSTIC MODEL

Our model is based on previous work by [7, 8] where a one dimensional transmission line model was developed to analyze lossy multilayered transducers. Salient features of this model include closed-form expressions for acoustic velocities and electric impedances of the piezoelectric element, valid in any one-dimensional system with losses. In the model [7] there is also no need for a non-intuitive negative capacitance $-C_o$ as used in the Mason equivalent circuit [9] and KLM [10] models for thickness vibrating piezoelectric elements. The approach is valid for thickness or shear vibrating elements as discussed in [7].

The complex effective impedance $Z_e^*(\omega)$ of the piezoelectric element is given by [8]:

$$\frac{1}{j\omega C_0} + \frac{|h_{33}|^2}{\omega^2 A}\left(\frac{2[\cosh(\gamma a)-1]Z_f + (Z_L+Z_R)\sinh(\gamma a)}{\left(Z_L Z_R + Z_f^2\right)\sinh(\gamma a) + Z_f(Z_L+Z_R)\cosh(\gamma a)}\right) \quad (1)$$

where Z_f^* is the impedance of the piezoelectric film, γ is the complex propagation constant, ω is the angular frequency, a is the thickness of the piezoelectric element, $h_{33} = e_{33}/\varepsilon_{33}^*$ is the piezoelectric stress constant, A is the transducer area, $C_o = \varepsilon_{33}^s A/a$ is the clamped electrical capacitance at constant relative displacement S. The acoustic impedances $Z_L^*(\omega)$ and $Z_R^*(\omega)$ are the combined impedances seen below and above the piezoelectric element, respectively.

The combined impedance $Z^*(\omega)$ for an arbitrary number of layers is computed using the impedance addition rule derived from transmission line theory. The complex transformed impedance at distance $d=L-x$ by a layer is given by:

$$Z^*(\omega,x) = Z_i^*(\omega)\frac{Z_{LD}^*(\omega)\cosh[\gamma(L-x)] + Z_i^*(\omega)\sinh[\gamma(L-x)]}{Z_i^*(\omega)\cosh[\gamma(L-x)] + Z_{LD}^*(\omega)\sinh[\gamma(L-x)]} \quad (2)$$

where γ is the complex propagation constant $Z_{LD}^*(\omega)$ is the load impedance, $Z_i^*(\omega)$ is the impedance of the intermediate layer, and L is the thickness of the intermediate layer. In general, $Z^*(\omega,x)$ is complex, except where $\gamma(L-x) = 0$ or $\pi/2$ (mod π). We can now compute the impedances $Z_L^*(\omega)$ and $Z_R^*(\omega)$ resulting from any number of piezoelectric or non-piezoelectric layers, inserting the results into (1) to obtain the effective impedance of the structure.

4 RESULTS AND DISCUSSION

With the transducers created using the fabrication scheme shown in Figure 1a, the piezoelectric coefficient of the PZT was found to be 80nm at 16V. A hydrophone (ONDA, Sunnyvale, CA) was used to measure the pressure transduced into a drop of water sitting on top of the electrode substrate. Initial experiments with a hydrophone showed that the PZT was generating pressures of 10^4 from

100-500kHz and 10^3 from 500kHz-1MHz. For the 500µm thick PZT disc samples, the model described in the previous section and the experimental data taken with an impedance analyzer predicted a resonant frequency around 4MHz (see Figure 4). The model predicts impedance values slightly higher than those measured experimentally due to secondary acoustic losses through the transducer. For instance, since this model predicts transducer performance only in one dimension, it does not account for losses in the other two.

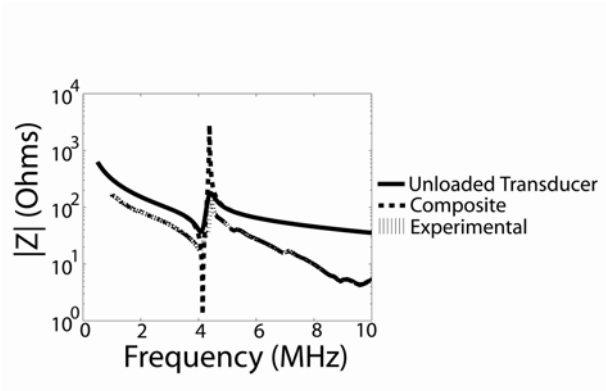

Figure 4. Modeled and experimental data for the transducer fabricated using the technique in Figure 1b. The curves for the unloaded transducer and the composite show the output of the model for the case in which the transducer is free standing and for the transducer with electroded surfaces. The experimental values were taken with an impedance analyzer.

For the systems created using the fabrication scheme shown in Figure 1c, the model and our experimental parameters show that the resonance of the PZT occurs close to 3MHz (see Figure 5). In order to avoid unwanted phenomenon such as acoustic streaming, the system was operated away from this point. We chose frequencies around 1MHz to better understand the behavior of the lateral mode excitations that are generated by the PZT. While the one dimensional model suggests that these modes exist, it does not predict how these modes will excite the particles in the cavity. These initial experiments were meant to characterize the system responses around this operating point.

In this system, the PZT electrodes were driven using a function generator with a 1MHz, 10Vp-p sinusoidal signal. Then particles were loaded into the microchannel using a syringe pump. Once loading had completed, the PZT was actuated and allowed to focus the particles in a plane close to the floor of the channel. In this system, both lateral

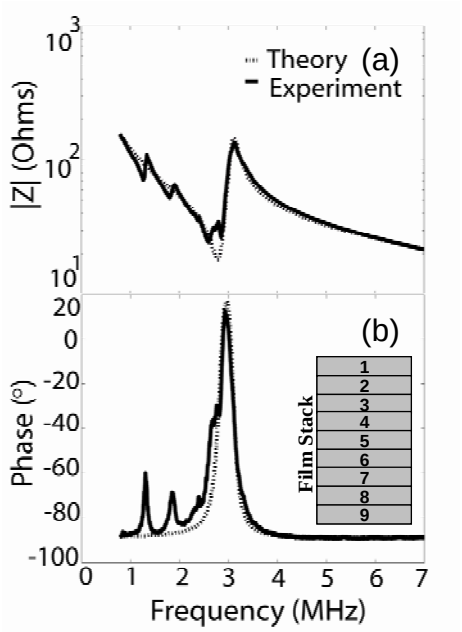

Figure 5. Model and experimental data for the acoustic system fabricated using the technique shown in Figure 1c. (a) Electrical impedance magnitude and (b) phase of the composite BM400 PZT transducer with water in the microchannel. Inset shows stack of materials for the generation of a standing wave in the acoustic manipulation system. (Each layer is as follows: 1. air 2. borofloat glass reflector, 3. microfluidic channel, 4.silicon substrate, 5. glue, 6. electrode, 7. PZT, 8. electrode, 9. air).

focusing and levitation were achieved due to standing waves set up from the primary acoustic field (along the height of the channel) and due to secondary coupling along the width. Excitation along the height of the channel can set up standing waves in another cavity dimension due to the anisotropy of the PZT and the resultant coupling of acoustic energy from one direction into another. The PZT was actuated at 1.12MHz, 12.22Vp-p for two flow streams and a gradual increase in frequency increased the number of flow streams (see Table 1). Figure 6 shows three flow

Table 1. Bead focusing characteristics during PZT actuation (number of experiments=6)

Frequency of Operation (MHz)	Amplitude of Applied Voltage (V) (peak-to-peak)	Number of Streams	Average Stream Width (µm)	Average Levitation Height (µm)
1	10.17	1	20±3	12±3
1.12	12.22	2	15±3	24±2
1.23	12.32	3	6±1	22±7

Values are mean±standard error of measurement.

streams generated due to operation at 1.23MHz, 12.32Vp-p. The concentration of particles injected into the device was 1% (v/v), and the maximum concentration of particles undergoing acoustic manipulation approached 90% (v/v), giving a preconcentration factor of 90x. At certain frequencies, unwanted cross nodes were generated along the length of the channel, resulting in inefficient focusing of the beads into separate streams. Slowly increasing the frequency from 1MHz to 5MHz resulted in data points that changed from a multi-node system to cross node frequencies where beads were oriented haphazardly in the channel. Also, above 20Vp-p, particles exhibited the phenomenon of acoustic streaming and would tend to agglomerate.

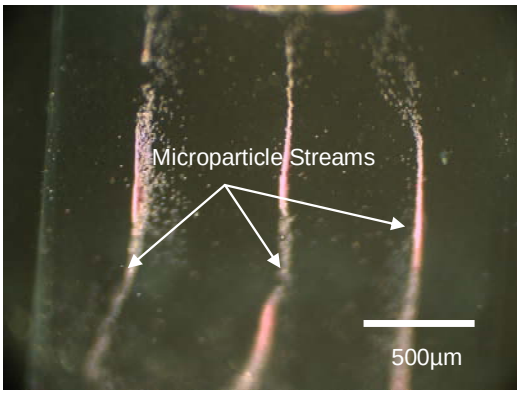

Figure 6. Acoustic focusing and levitation of 20µm particles in a 2mm wide, 100µm high microchannel.

5 CONCLUSIONS

In this paper we present data on the fabrication, modeling, and characterization of devices that integrate microacoustics with microfluidic systems to focus particles for flow cytometry applications. These systems allow for the creation of standing waves between the boundaries of microchannels to move particles to pressure nulls. By increasing the number of patterned top electrodes interfacing with the microfluidic channel as shown in Figure 2, we aim to "phase" the acoustic radiation force between two or more strips of electrodes together to achieve more reliable and complicated manipulation of microparticles. By understanding the complex distribution of radiation forces within the system in future work, we will be able to better predict the performance of these devices.
In the end, this integrated fabrication scheme has the potential to simultaneously increase functionality and portability while reducing system cost.

REFERENCES

[1] D. Huh, H. Wei, J. B. Grotberg, and S. Takayama, "Development of stable and tunable high-speed liquid jets in microscale for miniaturized and disposable flow cytometry," presented at IEEE-EMBS Special Topic Conference on Microtechnologies in Medicine & Biology, Madison, WI, 2002.

[2] R. Yang, D. L. Feeback, and W. Wang, "Microfabrication and test of a three-dimensional polymer hydro-focusing unit for flow cytometry applications," *Sensors and Actuators A*, vol. 118, pp. 259-267, 2005.

[3] C. Simonnet and A. Groisman, "High-throughput and high resolution flow cytometry in molded microfluidic devices," *Analytical Chemistry*, vol. 78, pp. 5653-5663, 2006.

[4] S. K. Ravula, D. S. Lidke, J. M. Oliver, D. W. Branch, G. Kaduchak, C. D. James, and I. M. Brener, "A microfluidic platform with microacoustics and dielectrophoresis for high throughput analyses of spatiotemporal signaling in biological cells," presented at Transducers, Lyons, France, 2007.

[5] S. K. Ravula, K. M. Taylor, D. S. Lidke, J. M. Oliver, C. D. James, and I. Brener, "A microfabricated flow cytometry system for optical detection of cellular parameters," presented at Biophysical Society Meeting, Baltimore, MD, 2007.

[6] S. K. Ravula, D. W. Branch, C. D. James, G. Kaduchak, M. Ward, M. Hill, and I. Brener, "A microfluidic particle manipulation system combining acoustic and dielectrophoretic particle preconcentration and focusing for miniaturized cytometry," submitted to IEEE Transactions on Biomedical Engineering.

[7] J.-L. Dion, "New transmission line analogy applied to single and multilayered piezoelectric transducers," *IEEE Transactions on Ultrasonics, Ferroelectrics, and Frequency Control*, vol. 40, pp. 577-583, 1993.

[8] J.-L. Dion, E. Cornieles, F. Galindo, and K. Agbossou, "Exact one-dimensional computation of ultrasonic transducers with several piezoelectric elements and passive layers using the transmission line analogy," *IEEE Transactions on Ultrasonics, Ferroelectrics, and Frequency Control*, vol. 44, pp. 1120-1131, 1997.

[9] W. P. Mason, "Physical Acoustics." New York: Academic Press, 1964.

[10] R. Krimholtz, D. A. Leedom, and G. L. Matthaei, "New equivalent circuit for elementary piezoelectric transducers," *Electronics Letters*, vol. 6, pp. 398-399, 1970.